JET–R(97)04

High Heat Flux Exposure Tests on Monoblocks Brazed to a Copper Swirltube

H D Falter, D Ciric, D J Godden, C Ibbot

JET Joint Undertaking, Abingdon, Oxfordshire, OX14 3EA, UK.

January 1997

SUMMARY

Actively cooled Beryllium Monoblocks brazed to a copper heat sink have been exposed to power densities of 20 - 25 MW/m^2 for up to 9 seconds. The beryllium, molten during exposure, stays on the tiles forming a smooth meniscus. The estimated melt depth is up to 3.5 mm. The uncastellated tiles showed deep cracks after approximately 30 pulses with surface melting. The castellated tiles sustained in excess of 100 similar pulses without visible cracking. Surface temperature and sublimation rate achieve equilibrium 3.5 seconds after the start of exposure for the uncastellated tiles. The castellated tiles, optimised to reduce thermal stress, have higher surface temperatures due to a lack of conducting cross section.

1.0 INTRODUCTION

Previous tests on 10 mm thick Be blocks brazed to a vapotron showed that the braze could withstand power densities up to 20 MW/m^2 for 2 s which brings the surface above liquidus for almost one second. The melting was approximately 0.7 mm deep and vertical cracks were found over a depth of up to 1 mm from the surface. After the test it was found by ultrasonic examination that the tiles had lost contact along the edges while the central part of the braze kept good thermal and mechanical contact [1].

The present test uses Be monoblocks with a slightly curved (r = 41 mm) surface and with a similar thickness (10 mm) of Beryllium as in the previous test. In previous tests with CFC monoblocks we found considerable variations in surface temperature from tile to tile which could be explained by variations in thermal conductivity of the tile material or by cracks in the CFC after the brazing. We observed however no deterioration of the tile surface tempertaure with the number of exposures. This led to the conclusion that the braze between cooling channel and CFC was very strong and essentially unbreakable [2, 3].

2.0 EXPERIMENTAL TEST DETAILS

The test was performed in the JET Beryllium test rig which has been previously described [1]. The test section is detailed in table 1 and is shown in Fig. 1. The beryllium monoblocks are brazed to a copper cooling pipe using InCuSil and an induction braze desribed in [1].

Table 1: Test section details

Be tiles	27 x 25 x 12 mm^3, uncastellated, Beryllium grade S65C
Braze cycle	Induction braze at 720^{o}C with InCuSil “ABA” braze
Heat sink	1 mm thick, 10 mm i.d. copper pipe with 1mm thick swirl Ribbon with 360^{o} twist in 40 mm.
Water flow rate	4 - 4.3 m^3/h - corresponds to16 - 17 m/s
Water inlet temperature	20^{o}C
Water pressure	Approximately 6.6 bar in the test section
Water pressure drop	5.3 bar

2.1 Test sequence

Table 2: Test sequence

Part 1 - T_s<1250^{o}C	10 pulses with 7 sec duration at 5 MW/m^2 and at 7 MW/m^2
Uncastellated	160 pulses with 6 sec duration at 10.5 MW/m^2.
Monoblock	Calibration of the IR imaging system
Old calorimeter	Visual examination of the test section
Part 2 - T_s>1250^{o}C	10 pulses with 2.4 sec duration and 13.7 MW/m^2
	Modulated pulses with 3 s at 6.7 MW/m^2 followed by up to 2s at 20 - 22 MW/m^2. 20 Pulses with surface melting. Visual examination of the test section and installation of a copper calorimeter with higher heat capacity.
Part 2a	Implantation test with 5 MW/m^2 Beryllium beam - 80 pulses 6s duration see separate report [4]
Part 3;	large calorimeter Exposure to 20 MW/m^2 for up to 9s. 25 pulses with surface melting. Total time above liqiudus 65s, max. in one pulse: 7.8s
Part 4: castellated	Monoblock 130 significant pulses with above 15 MW/m^2 for more than 2.5 seconds

The test was carried out in four parts with a visual examinations of the mock-up and some modifications of the set-up in between. The detailed sequence, listed in Annex 1 - 3 , is shown in Table 2.

2.2 TEST GEOMETRY

The test section was installed vertically behind a scraper with the outer 3 mm of the test section shielded by one of the scrapers. A copper calorimeter with 16 mm spacing between the individual calorimeter blocks was installed beside the test section and used for measuring the vertical profile and the power density. Both test section and copper calorimeter, are inclined by 75^{o} against the beam normal. A schematic plan view of this experimental set-up is shown in Fig. 2a.

For parts 3 and 4 of the experiment the new copper calorimeter with increased heat capacity was installed behind the test section as shown in Fig. 2b .

2.3 DIAGNOSTICS

The surface of the test section is viewed by an IR imaging system and by a video camera. The IR system can either run in frame mode with a repetition rate of up to 30 Hz or in line mode with a repetition rate of up to 2.5 kHz. Most of the measurements were done in frame mode. The highest calibrated range is 500 - 2000^{o}C which allows measurements above 2000 ^{o}C for emissivities < 1. In this high temperature range a narrow bandwidth filter is used with maximum transmission at 2.8 micron. The viewing angles are shown in Fig. 3 which gives the side view of the test rig .

For the shots with surface melting an optical diagnostic to measure the intensity of the BeI line ($2p^1P^0$ - $3d^1D$ at 4573 Å) was installed at the bottom window and a miniature CCD camera was used at the top window together with the IR imaging system.

Power density is measured with both an inertial copper calorimeter and water calorimetry. In the case of water calorimetry we measure the absorbed total energy E_{tot} and get the peak power density $p_{max.}$ via

$$E_{tot} = p_{\max} \times w \times \tau \times \int p(z) / p_0 dz$$

with w = exposed width of the test section, τ = exposure time, and $p(z)/p_0$ as normalised vertical power density.

It should be noted that both measurements give a power density averaged over the width of the test section. The accuracy of the power density measurement depends on the knowledge of the exposed width of test section and calorimeter, which can not be measured in situ because of the Beryllium contamination. In this report we take the relative width of both from in situ video prints and scale this width to a total of 50 mm, which is the measured gap between the two scrapers. The best guess for the power density is then the average of water calorimetry on the test section and inertial calorimetry, thus averaging out the error in the individual width of the components.

Every second tile is instrumented with a chromel alumel thermocouple as shown in Fig. 1. Typical thermocouple traces are shown in Fig.4.

2.4 POWER DENSITY PROFILE

The vertical profile can be derived from the inertial calorimeter. Fig. 5 gives an example for a pulse with steady state conditions (7s) and modest power densities (7.45 MW/m^2). The profile is well fitted by a gaussian distribution with 90 mm e-folding length with an added flat top of 10 mm width. The power density in the centre stays above 90% of the peak power over the width of 6 tiles.

The horizontal profile is normally derived from the surface temperature distribution. In this test with curved tiles in the horizontal plane this is not possible. From previous test we can assume that the power density peaks at the exposed edge of the test section (which is in the beam centre) and falls by approximately 20% over the width of the tile in the direction to the scraper.

The power density from water calorimetry and from the inertial calorimeter agree generally quite well (Fig. 6a) with a scatter of 6%. In parts 3 and 4 with the larger calorimeter the difference increases to 25% (Fig. 6b).

2.5 BEAM PROPERTIES.

The tiles were exposed to a hydrogen beam with an energy of 52 ±10 keV/amu in the full energy component. The beam is approximately 60% neutralised with roughly 44% of the power in full energy particles, 44% in particles of 1/2 and 1/3 of the full energy and 12% in impurities. The gas used for the hydrogen beam is partially recirculated inside the vacuum chamber and is probably contaminated with oxygen. The oxygen flux in the beam is approximately 6% of the total flux as derived from the doppler shifted intensity of hydrogen with 1/19 of the total energy (H_3O^+) (Fig. 7). The pressure in the vacuum chamber during exposure is approximately 4 μbar.

2.6 BEAM MODULATION.

The power density in the beam is basically constant during a pulse. The average power density on the test section can be varied by modulating the beam (on/off modulation). The modulation sequence used for the second part of this test was:

- Modulation with 32ms on every 94 ms for 3 seconds (average power density is 33% of the peak power density) followed by
- beam full on for up to 2 seconds.

The calibration of the IR imaging system was done at the end of part one and gave an emissivity of 0.62. As observed previously [1], Beryllium darkens considerably with exposure, in particular when the surface temperature approaches liquidus. Consequently the absolute value of the surface temperature is only correct if the emissivity has been measured shortly before or after the respective pulse. Another drastic change in emissivity down to 0.1 occurs when the surface has been long enough above liquidus.

3.0 EXPERIMENTAL RESULTS FOR PULSES WITHOUT MELTING

The experimental results are listed here in sequential order.

3.1 Thermal characteristic of the tile

The surface temperature, taken as average in a small area at the hottest tile is shown in Fig. 8 for 6 and 7 second pulses at 5, 7.1 and 10 MW/m^2. The emissivity, shown in the legend, has to be increased as the test progresses to give matching temperatures. In particular the two pulses at the beginning (87808) and at the end (88071) of the 160 10 MW/m^2 pulses require emissivities of 0.41 and 0.62 to give the same surface temperature. The power density shown is the average between inertial and water calorimetry and the difference is within the data scatter.

The thermocouples in the Be tiles show that the power loading is practically constant for the 7 tiles in the centre (Fig. 9). The maximum TC temperature rises linearly with power density. Comparing the two 10 MW/m^2 pulses of Fig. 8 shows the good reproducibility (the 7s pulse has slightly higher temperatures).

The surface temperature distribution at the end of the 10 MW/m^2 cycling (pulse 88071) is shown in Fig. 10. The surface temperature follows the curvature of the surface without hot spots and is remarkably smooth. The measurement uses the emissivity of 0.62 from the IR calibration done immediately after this pulse. The highest surface temperature in this part of the test was

1250 ^{0}C, just below the liquidus. The surface had been cycled between room temperature and above 1000 ^{0}C in 127 pulses.

3.2 IR calibration

The calibration of the IR imaging system was done by heating the test section without cooling to approximately 600 ^{0}C. During the following cooldown the emissivity required to get the same temperature on the surface as measured by the thermocouple was calculated in steps of 10 degree. The result is shown in Fig.11. The emissivity is constant at 0.62 in the range between 600 and 300 ^{0}C.

3.3 Visual examination.

After a total of 190 pulses of more than 1s exposure and 127 pulses with surface temperatures in excess of 1000 ^{0}C the test section was pulled out of the vacuum tank and photographed. Due to health physics restrictions the examination was limited to pictures taken from a distance of 1 meter and to an endoscopic examination. Figure.12 shows photographs of the test section and Fig. 13 shows a pictures from the endoscope. No damage or cracks are observed on the test section. At this stage we also removed a disc holder installed at the picture frame scraper facing the test section. The disks and the holder are clearly discoloured (Fig. 14).

4.0 Pulses with surface melting

In this part of the test the beam power is set to 21 MW/m^2. For the first 5 seconds (3 seconds later in the test) the power density is reduced to 1/3 by modulation. After that the tiles are exposed to the full power density of 21 MW/m^2 for up to 1.9 seconds. The total number of theses pulses was 21. The sequence is set up to model a power excursion in a fusion device.

4.1 Redeposition of Beryllium on the copper calorimeter.

The first observation was a discoloration of the copper calorimeter which was initially believed to indicate surface melting on the copper calorimeter (Fig. 15). To reduce the loading of the calorimeter we shortened the length of the modulated exposure from 5 to 3 seconds. Later it became clear that we actually observed redeposition of Beryllium onto the copper. This redeposition is only significant when the surface temperature of the Beryllium tiles is above liquidus. It is remarkable that the redeposition takes place in the high power density area and that the redeposited material is solidly attached as will be shown later. At the end of the experiment the Beryllium layer on the copper calorimeter looked quite substantial and indeed the copper calorimeter looks the same as the Beryllium monoblocks (Fig.16). The Beryllium is firmly attached to the copper base and does not show hot spot. This can be seen in Fig. 17 which shows the surface temperature distribution during beam on in a 11 MW/m^2 pulse (#88165) on the

coated copper calorimeter. The spikes on the vertical profile are the slots between the individual copper blocks. The temperature shown in Fig.17 is too high as the emissivity of the IR system was set to 0.1, as required for the molten part of the monoblock. The same conclusion can be drawn from Fig 18 taken with the CCD camera with a higher spatial resolution. Hot spots are mainly concentrated in the casetellations between the tiles and not on the surface.

At this point we decided to interrupt the experiment in order to examine the thickness of the Beryllium on the copper calorimeter. However, in a final 9 second reference pulse the actual power density was 11 MW/m^2 well above the intended power density of 7 MW/m^2 and this caused substantial melting on the copper calorimeter which removed the Beryllium deposit (Fig. 19). The component was removed to fit a new copper calorimeter with higher heat capacity.

4.2 Tile damage

The Beryllium Monoblocks show clear surface melting on 10 blocks (Fig.19). The resolidified Beryllium forms a smooth meniscus. On the fourth tile from bottom, the lowest tile with melting, we find several cracks in the resolidified Beryllium (see blow-up in Fig.19). All the other tiles look perfect as demonstrated by the second blow-up in Fig.19. The resolidified surface is smooth, silvery grey and shows a high reflectivity.

4.3 Thermal observations.

The melting and in particular the recondensation of the beryllium is visual on the time plot of the surface temperature (Fig.20). By assuming that the temperature gradient through the liquid during recondensation can be neglected (beam is off) we can use this recondensation phase as calibration point and fix the emissivity to force the temperature to equal the transition temperature of 1287 ^{o}C. This is done in Fig. 20 for 4 small areas defined in the insert. The surface starts to melt 0.45 seconds after applying the full power density. 1.24 seconds after applying the full power density the surface appears to approach equilibrium at roughly 1900 ^{0}C. During cooldown a delay of approximately 0.45 seconds is observed due to resolidification (Fig. 21). From this delay we can estimate the thickness of the melt layer:

We assume that 12 MW/m^2 of energy is transported through the Beryllium into the water[1]. The delay in the cooldown allows to calculate the energy released by the resolidification. From the heat of fusion (1300 kJ/kg) we can now calculate the thickness of the melted layer. In the case of 12 MW/m^2 as conducted power and 0.45s of resolidification time we get a melt depth of 2.25 mm.

[1] The monoblocks can absorb almost 11 MW/m^2 in steady state. In the case of melting, the transition temperature of 1287 ^{0}C is below the surface. The thermal gradient through the Beryllium is larger than in the 11 MW/m^2 exposure and consequently heat transport is larger than 11 MW/m^2.

Without a unique emissivity over the surface of the Beryllium the output of the IR imaging system can be quite misleading. Fig. 22 shows the temperature distribution of the test section after melting of the surface and evaluated with an emissivity of 0.1. In total contrast to Fig. 10 we now see the edges (which means the non melted sections) of the tiles as the hottest areas (higher emissivity).

4.4 Evaporation rate of Beryllium

Both, surface temperature and Beryllium partial pressure appear to reach steady state approximately 1.5 s after the start of the full power density (Fig. 23). The surface temperature, again calibrated to 1287^{o}C at the recondensation plateau, is in this case approximately 2000K. For this temperature the evaporation rate is 5x10^{-2} gr/cm^{2} s [5]. With a heat of evaporation of 36600 J/gr. [6] this corresponds to an evaporation cooling of nearly 20 MW/m^{2}. As the evaporation rate rises steeply with temperature, it is sufficient to assume an error of 100K in the surface temperature to explain the observed steady state by the cooling effect of the evaporation.

5.0 Second test sequence with surface melting

In this test sequence we used the new calorimeter and we drop the initial modulation of the beam. The main parameters of the sequence are listed in Annex 2, power density and exposure time are shown in Fig.24. The surface temperature of the monoblocks was above melting temperature in 25 pulses.

5.1 Thermal observations

The longest pulse with 9 seconds of exposure is shown in Fig.25. Surface temperature and beryllium vapour pressure show equilibrium after 3.5 seconds. The thermocouple has a considerably longer time constant and the depth of the melted zone appears to increase with the square root of time (Fig.26). The corresponding melt depth is 3.5 mm for a recondensation time of 0.7 seconds. At this high surface temperatures and vapour pressures the coating of the windows with beryllium is likely to distort both: the temperature measurement and the measurement of the Beryllium line intensity as is demonstrated in Fig.27: The intensity of the Beryllium line drops from pulse to pulse particularly for the long pulses. The overall reduction is close to one order of magnitude.

Using the sublimation rate [5] with $$\Gamma = \frac{2.6 \bullet 10^{20}}{\sqrt{\mathrm{M} \bullet \mathrm{T}}}\ 10^{B - A/T,} \left[\frac{atoms}{cm^2 \bullet s} \right]$$

A=16720, B= 11.61, and M=9 for Beryllium we can compare our measured Be line intensity with the evaporation rate calculated using the measured surface temperature. The agreement is almost perfect (Fig. 28). This gives confidence, that the temperature measurement in this particular pulse is correct and that applying the sublimation formulae in numerical models as RACLETTE [7] is justified.

5.2 TILE INTEGRITY

The resolidified Beryllium is still firmly attached to the tiles forming a smooth meniscus. Two tiles show cracks across the full width of the block. The cracks are likely to be very deep, as in both cases a displacement of the tile edge is visible. There are also some smaller surface cracks mainly at the end of the melted zone (Fig.29).

6.0 CASTELLATED BERYLLIUM MONOBLOCK

This mock-up was designed to avoid stress concentration. The testing concentrated on exposure with surface melting to verify that it has a better crack resistance. The exposure statistics is shown in Fig.30 and Annex 3 and consisted mainly of about 20 pulses with a duration of 9 seconds and a power density 5-6 MW/m2 and approximately 30 pulses with 15 - 20 MW/m^2 and mostly 4 seconds duration, and finally 100 pulses at 20 MW/m^2 and 3.5 s duration.

6.1 THERMAL OBSERVATIONS.

As this design has less conducting material between surface and water channel (see Fig. 2 for cross section), the tile showed higher surface temperatures and sublimation rates. In fact the sublimation rate was so high that the windows were essentially covered during the first long pulse and meaningful optical measurements were impossible. Figure 31 shows that the measured surface temperature starts to fall rapidly 3.5 s after the start of the pulse. The extracted power is actually increasing and this drop in temperature demonstrates a loss of transmission due to coating of the window. We also see a change of slope in the tank pressure at this time - again an indication of the high Beryllium vapour pressure (gettering).

6.2 TILE INTEGRITY

As expected the surface shows quite heavy melting, but the recondensed Beryllium is still on the tile (Fig.32). On two castellations the liquid has merged together and lateron cracked probably during recondensation. Apart from this crack, there is no sign of surface cracking.

6.3 BERYLLIUM DEPOSIT ON THE COPPER CALORIMETER.

In sections 3 and 4 with the calorimeter behind the test section we find much lower beryllium deposited on the copper calorimeter. This proves, that the thick layer observed with the calorimeter at the same height as the Beryllium mock up and inclined against the mock up by 30 degree was direct deposition of evaporated material without contribution of the beam.

7.0 DISCUSSION

The quality of the bond of the redeposited Beryllium on the copper calorimeter is remarkable. The stability of the molten surface layer appears to be more stable on the Monoblock than on the Be tiles brazed to a vapotron [1]. This is probably caused by the overheating of the tile edges in the case of flat tiles.

Even after extended exposure and quite high surface temperatures we see no dripping from molten material. The mock up is installed vertically and is exposed to gravity and probably some vibration from the water flow. The micrographic examination of the melt depth and of crack propagation is outstanding and has to be organised by ITER or NET.

In the JET melt experiment [8] sweeping was stopped and the preheated inertial tiles were exposed for up to 4.5 seconds to nominally 25 MW/m^2. Melting with tile damage was observed and the molten Beryllium had splashed. From the existing data it can not be decided whether this splashing is caused by electromagnetic forces in the JET machine or if the fact that the tiles were uncooled was the decisive factor.

A comparable exposure to the JET melt experiment is pulse 88158 with 21 MW/m^2 and 3s of preheating (Fig.23) where Beryllium sublimation saturates 1.5 seconds after the start of full exposure. If we assume that 5 MW/m^2 is used up for sublimation in Fig. 23 we get a sublimation rate of 1.4 10^{-2} gr/cm^{2}s (1870 ^{o}K). This is a very substantial sublimation rate corresponding to a total sublimation of of $1.4 \cdot 10^{-2} \frac{gr}{cm^2 s} \cdot 1000 cm^2 \cdot 3s = 120 gr$ Beryllium in one JET pulse. From the erosion seen the JET divertor tiles after the melt experiment a sublimation rate of the order of 100 gr/pulse can not be ruled out.

REFERENCES

1 H D Falter et. al., “High heat flux exposure tests on 10 mm Beryllium tiles brazed to an actively cooled Vapotron made from CuCrZr”, JET-R((96)02

2 H D Falter et al, “Testing of plasma facing materials for divertors in the JET Neutral Beam Test Bed”, SPIE Vol. 1997 High Heat Flux Engineering II (1993) 170 - 181.

3 H D Falter et. el., “Comparison between Actively cooled divertor dump plates with Beryllium and CFC Armour”, Proceedings of the 18th Symposium on Fusion Technology (SOFT 18) held in Karlsruhe 22-26 August 1994 pp 291 - 294 also in JET-P(9440

4 H D Falter, D Ciric, J P Coad, D Godden, “Deuterium implantation inactively cooled Monoblocks”, Jet Report xxxx

5 R.A. Langley, J. Bohdansky, W. Eckstein, P. Mioduszewski, J. Roth, E. Taglauer, E.W. Thomas, H. Verbeek, K.L. Wilson, Data Compendium for Plasma-Surface Interactions - Chapter 5: Evaporation, Nuclear Fusion (1984).

6 ITER Beryllium database

7 A.R. Raffray, G. Federici, “RACLETTE: A Model for Evaluating the Thermal Response of Plasma Facing Components during Slow High-Power Plasma Transients - PART I, Theory and Description of Model Capabilities”, to appear in J. Nucl. Mat.

8 B Tubbing, “The operational characteristics of a molten and damaged beryllium divertor target in JET”, JET-P(95)

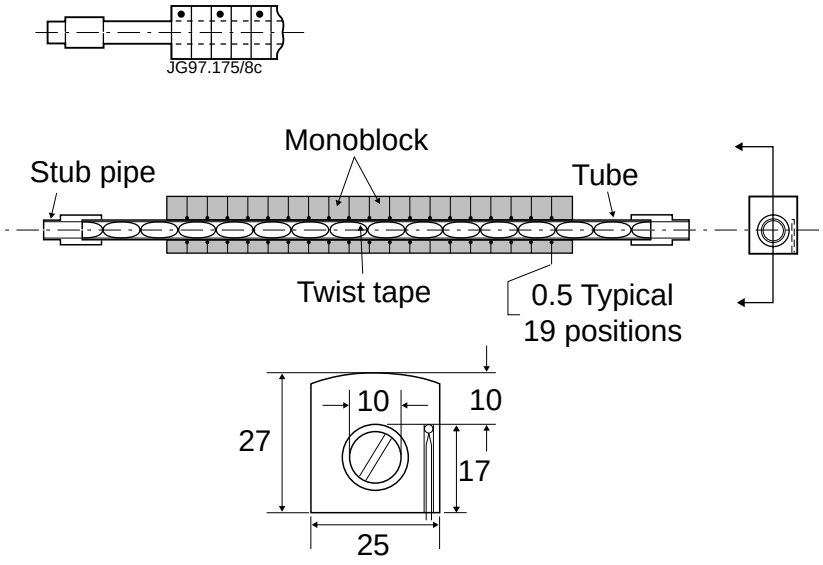

Fig.1: Cross section of the Beryllium monoblock test section. The individual monoblocks are 10 mm wide. The other dimensions are shown in the insert.

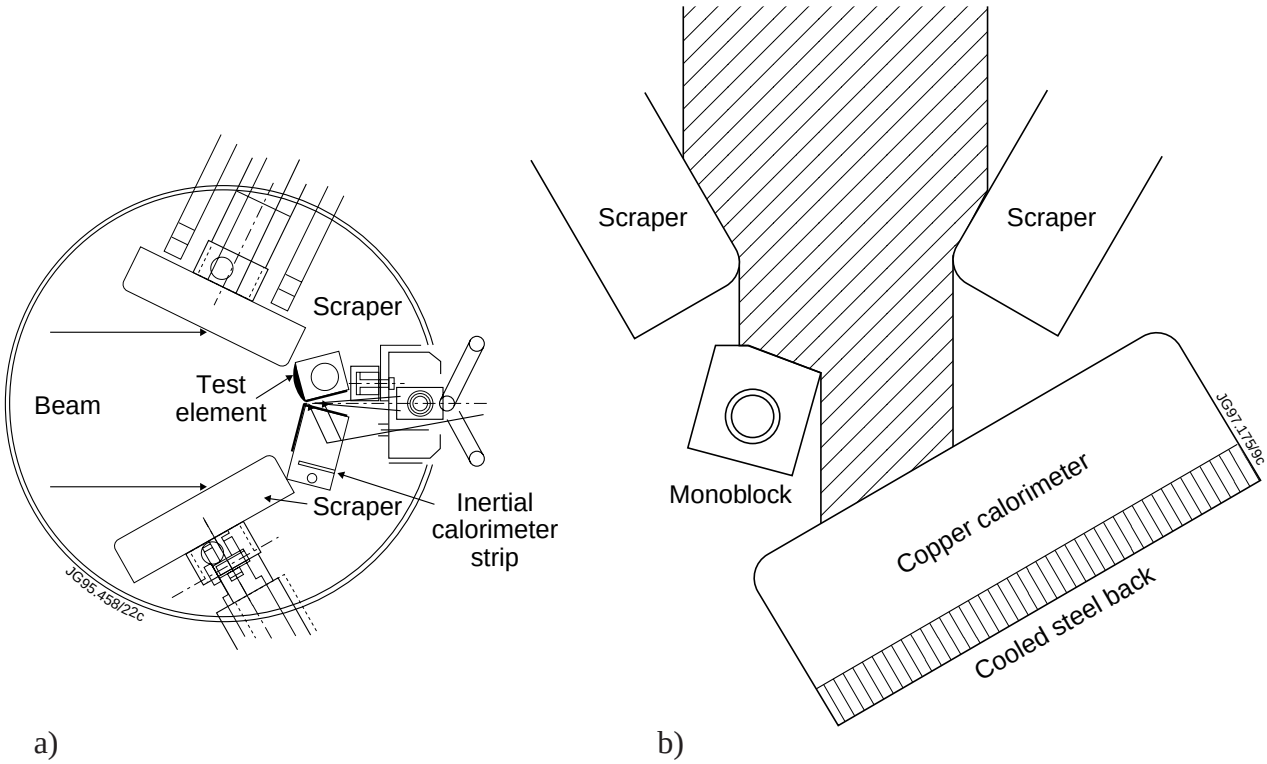

Fig.2: Plan view of the test set-up. The test section is installed behind vertical scrapers with a copper calorimeter array right next to the test section. a) initial set-up for parts 1 and 2, b) set-up for parts 3 and 4.

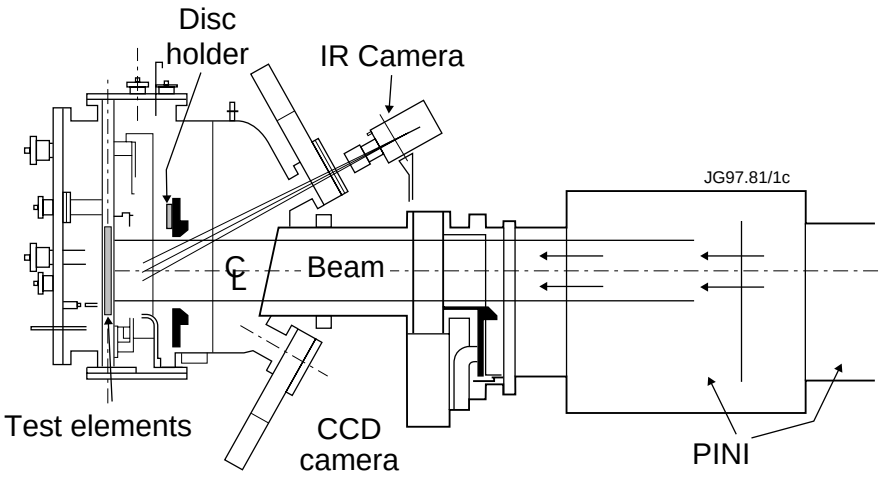

Fig.3: Elevation view of the Beryllium test rig. The test section is viewed by the IR imaging system and by a SVHS CCD camera under an angle of 30^o. The viewing field is limited top and bottom by scrapers. When the H_α diagnostic is in use IR and CCD camera use the top window and the H_α system uses the bottom window.

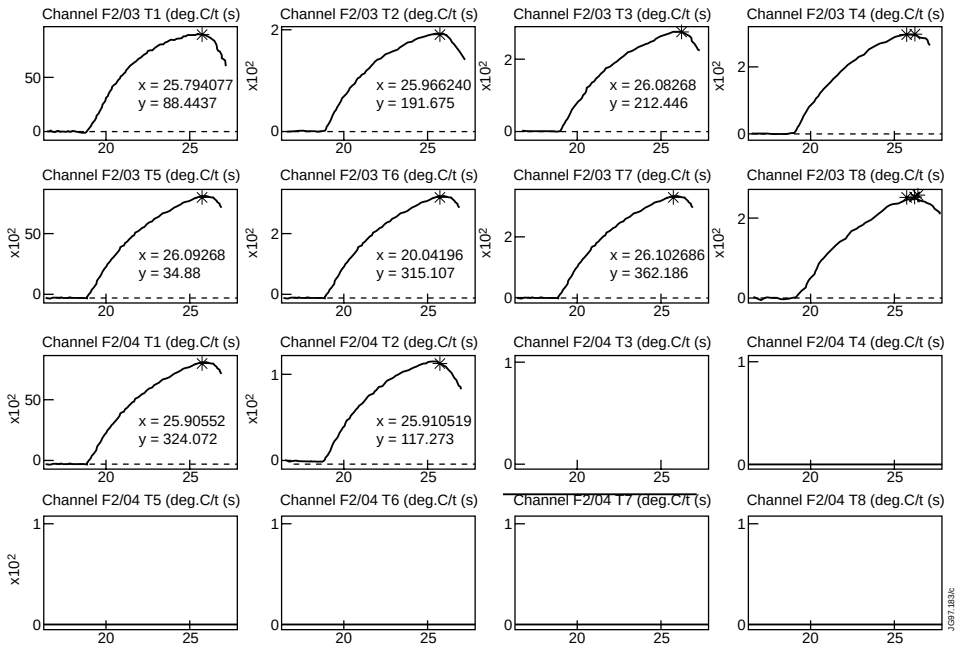

Fig.4: Thermocouple response in a 7 s pulse with 10 MW/m^2.

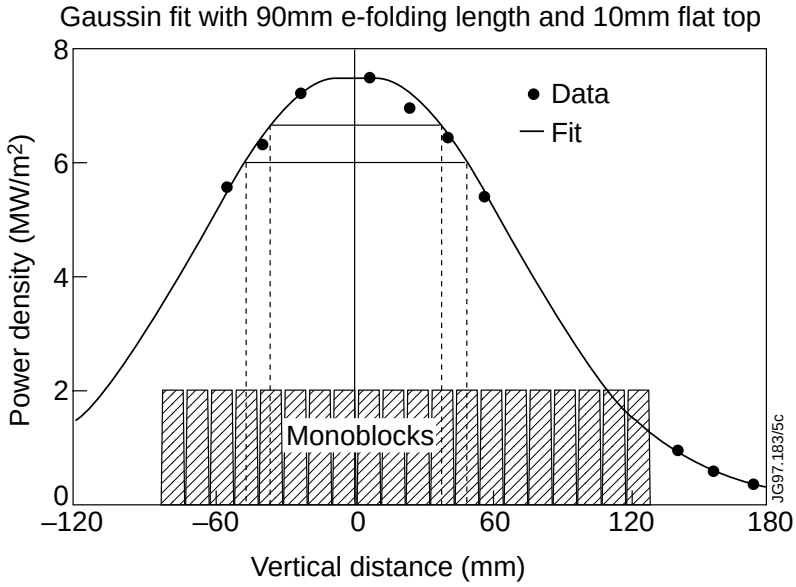

Fig.5: Vertical beam profile from the inertial copper calorimeter array.

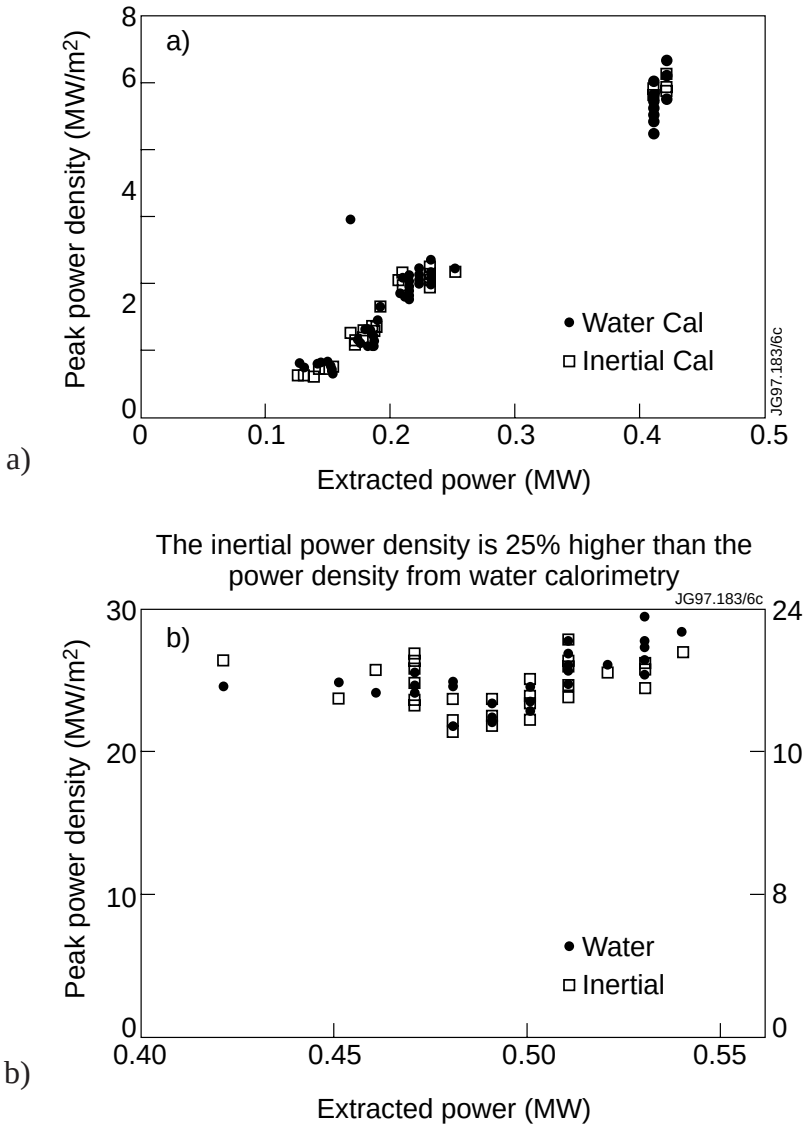

Fig.6: Power densities from inertial and water calorimetry. A): parts 1 and 2 with the calorimeter at the side of the monoblock, b): parts 3 and 4.

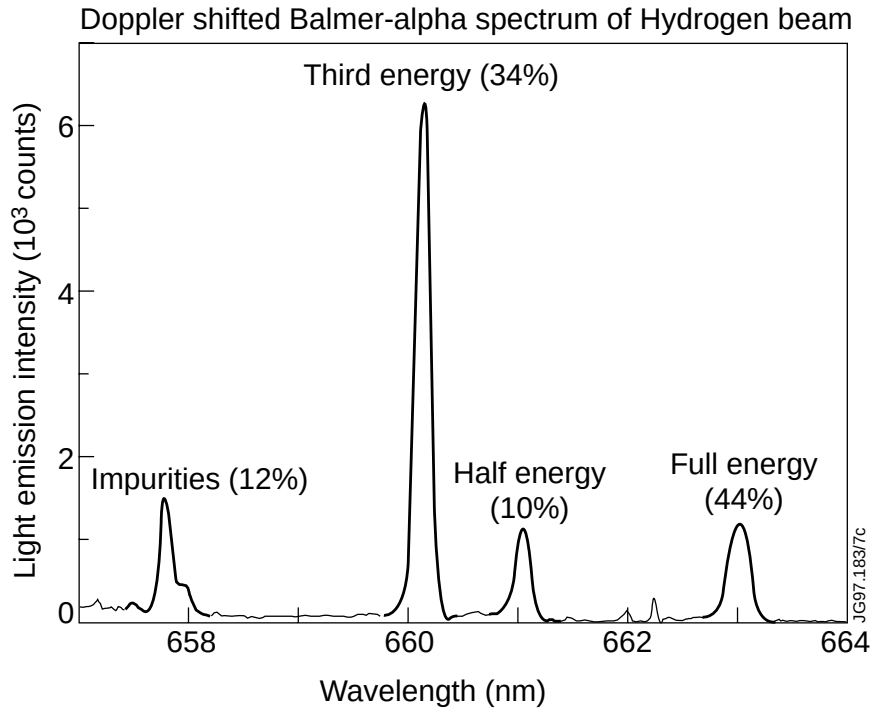

Fig.7: Typical beam composition in the Beryllium test rig from the doppler shift of the H_α line. The percentages shown are the power fractions. The impurities are mainly mass 19 (H_3O^+). The flux of oxygen is estimated at 6% of the total flux.

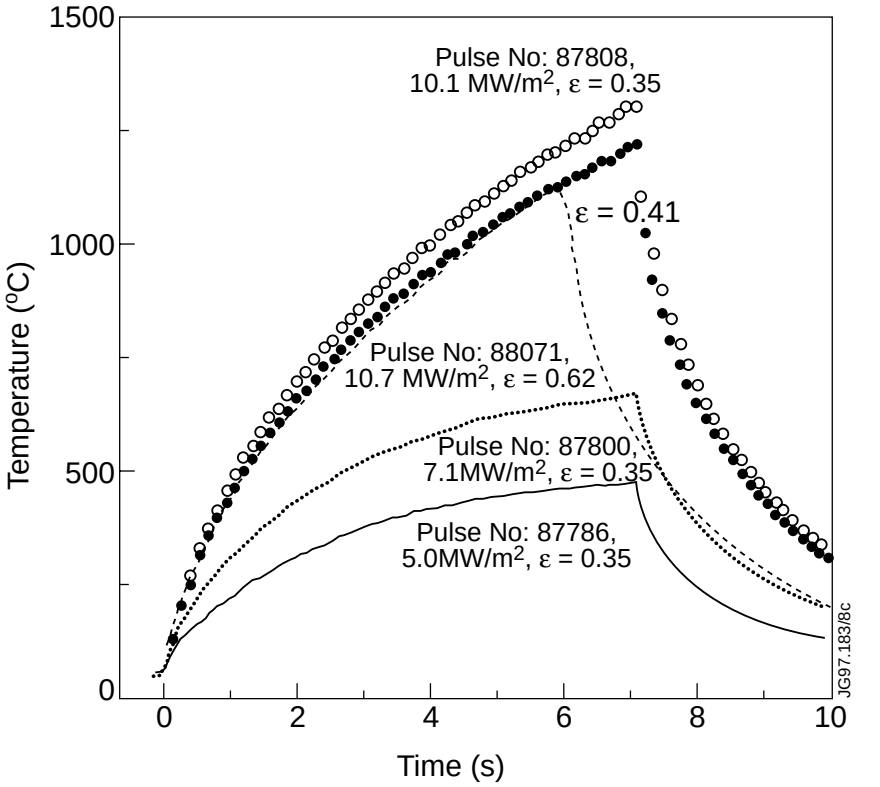

Fig.8: Maximum surface temperature on the hottest Beryllium monoblock. The last pulse (88071) was taken just before the calibration of the IR camera and uses the emissivity from the calibration. To match an earlier pulse at equal power (87808) a lower emissivity has to be used. The thermal time constant increases with power.

a) Max. temperature rises versus power density

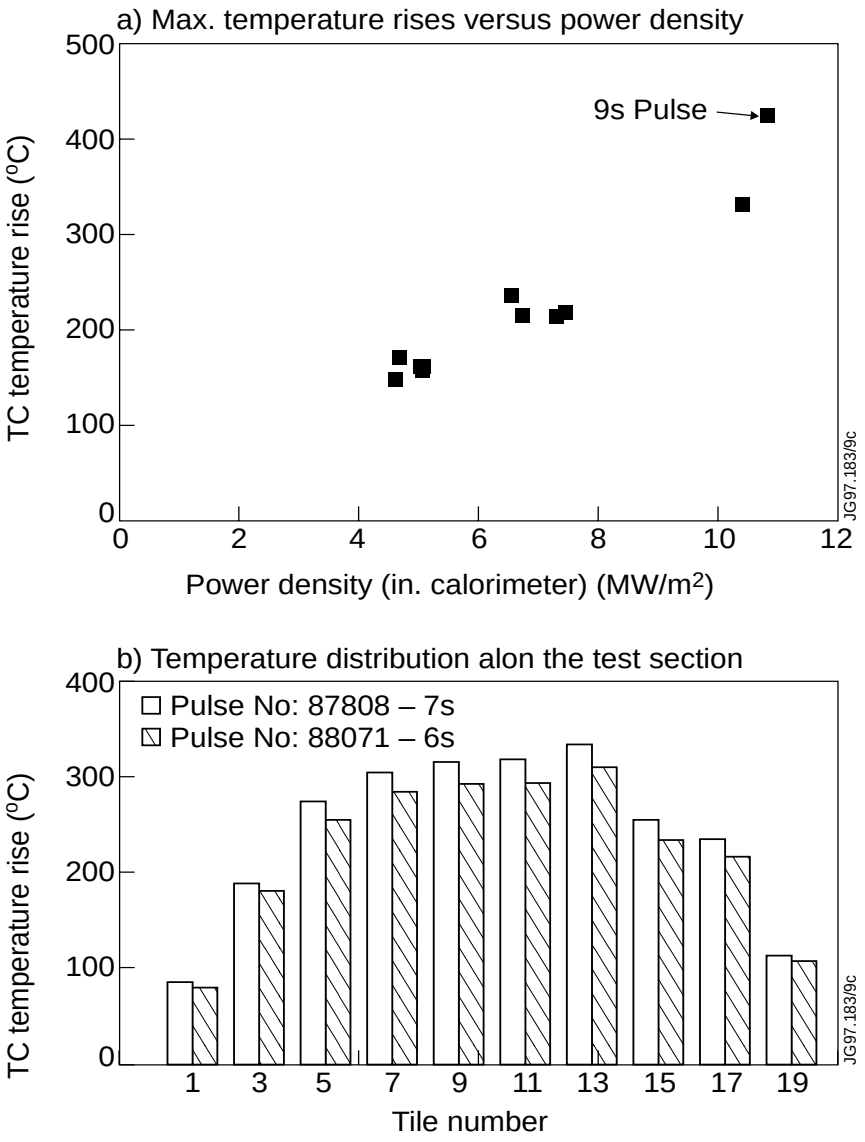

b) Temperature distribution along the test section

Fig.9: TC temperature 10 mm below exposed surface. The reproducibility is good. The 7 tiles in the centre show equal temperatures. The temperature increases linearly with power.

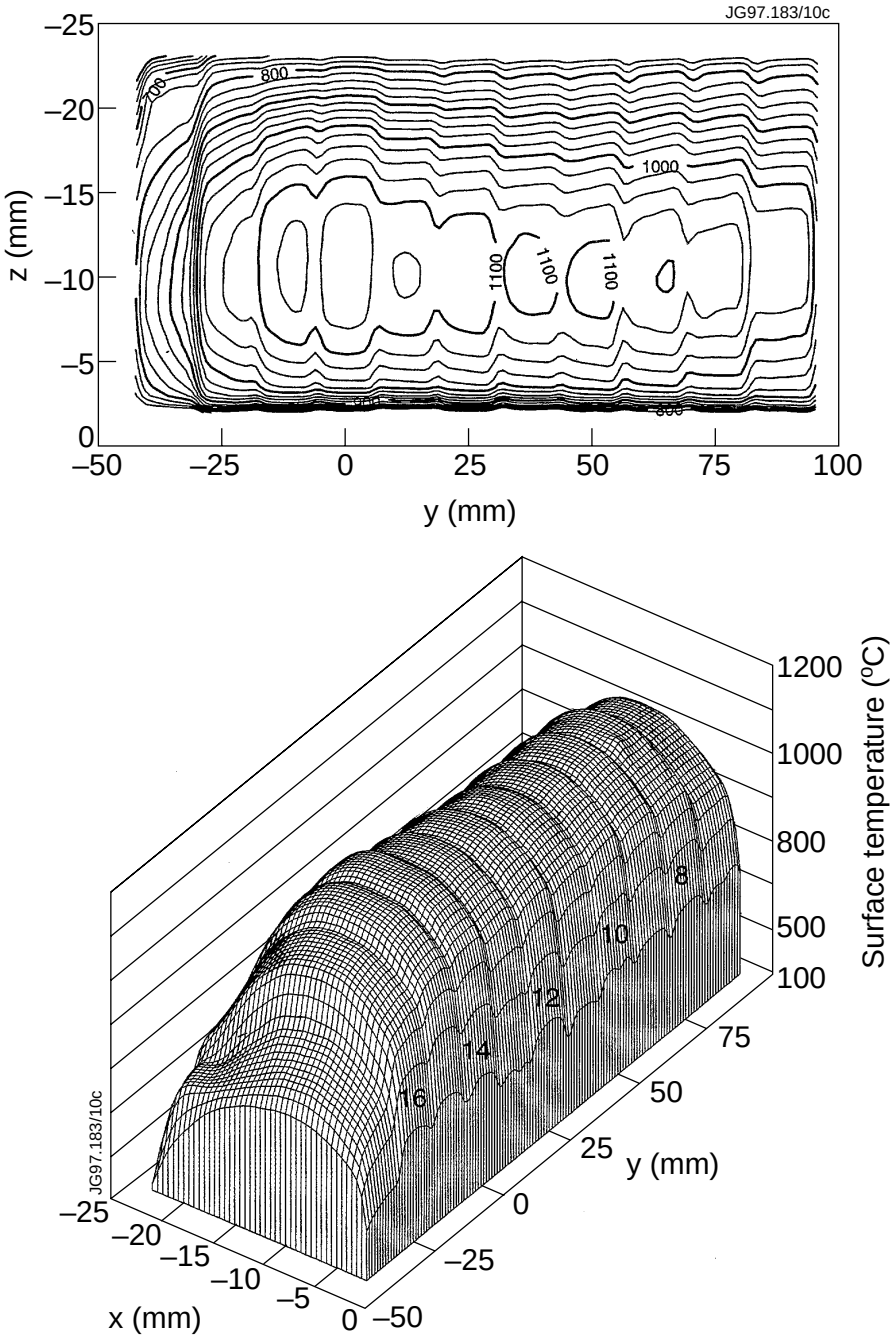

Fig.10: Surface temperature distribution of a 10 MW/m^2 pulse with 6s duration (pulse 88071, last frame with beam on)

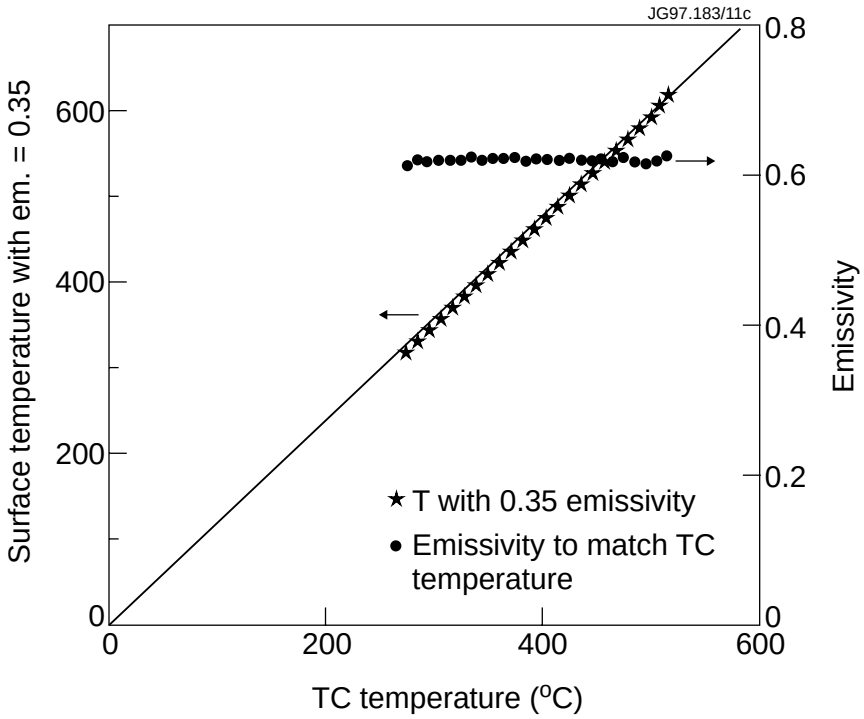

Fig.11: Emissivity from IR calibration

Fig.12: Photographs of the tile after part 1. Left: The discoloration of the Beryllium reflects the intensity of the exposure. The copper calorimeter shows substantial deformation and discoloration - probably Beryllium from previous tests. In this test there was no melting at the time this pictures were taken (end of part 1).

Fig.13: Tile surface after part 1 as seen by the endoscope. Note no visible cracks or melt marks.

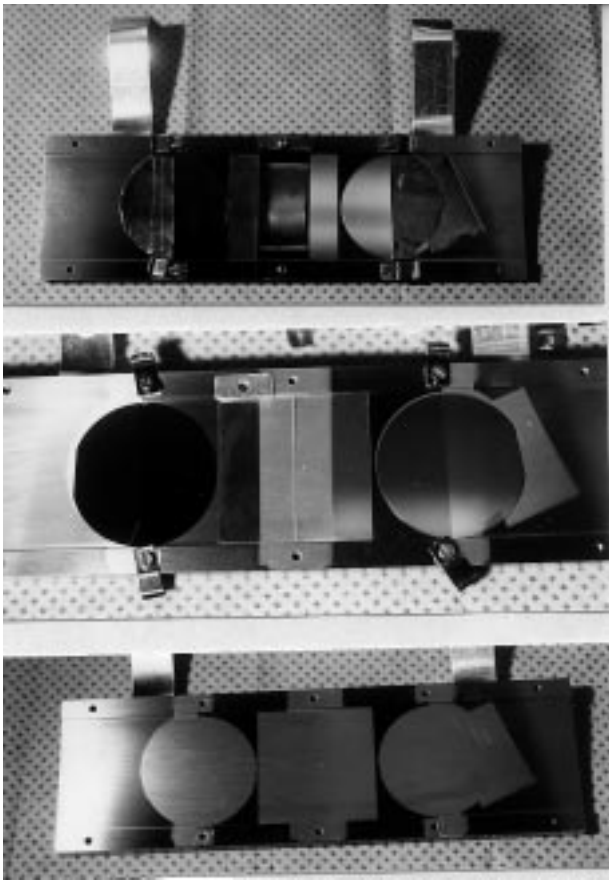

Fig.14: Disks and disk holders after part 1. The assembly was hanging on the top scraper in Fig. 3 (J96.236c/ 30, /8, /1)

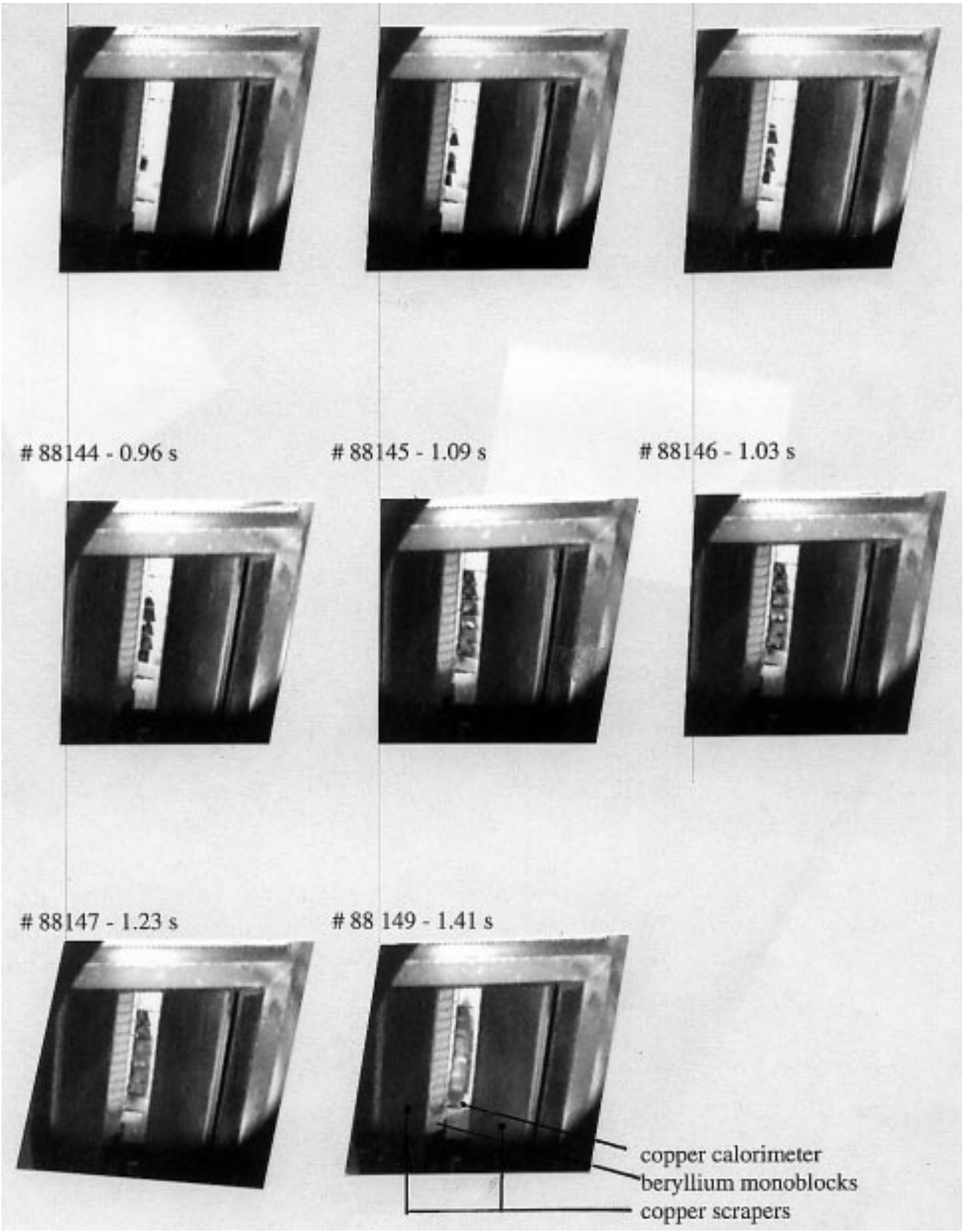

Fig.15: Covering of the copper calorimeter with Beryllium in pulses with surface melting. Shown is the pulse number and the unmodulated ontime at 20 MW/m^2.

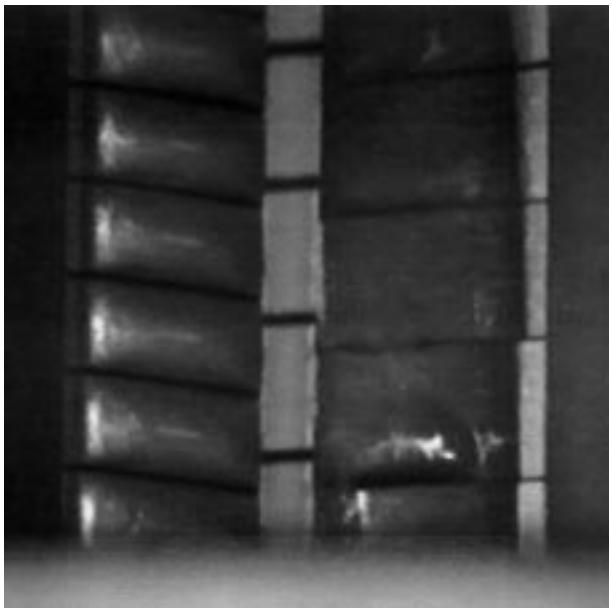

Fig.16: View on test set-up with Be monoblock test section at the left and the Be coated copper cal. on the right. Picture taken before the last pulse.

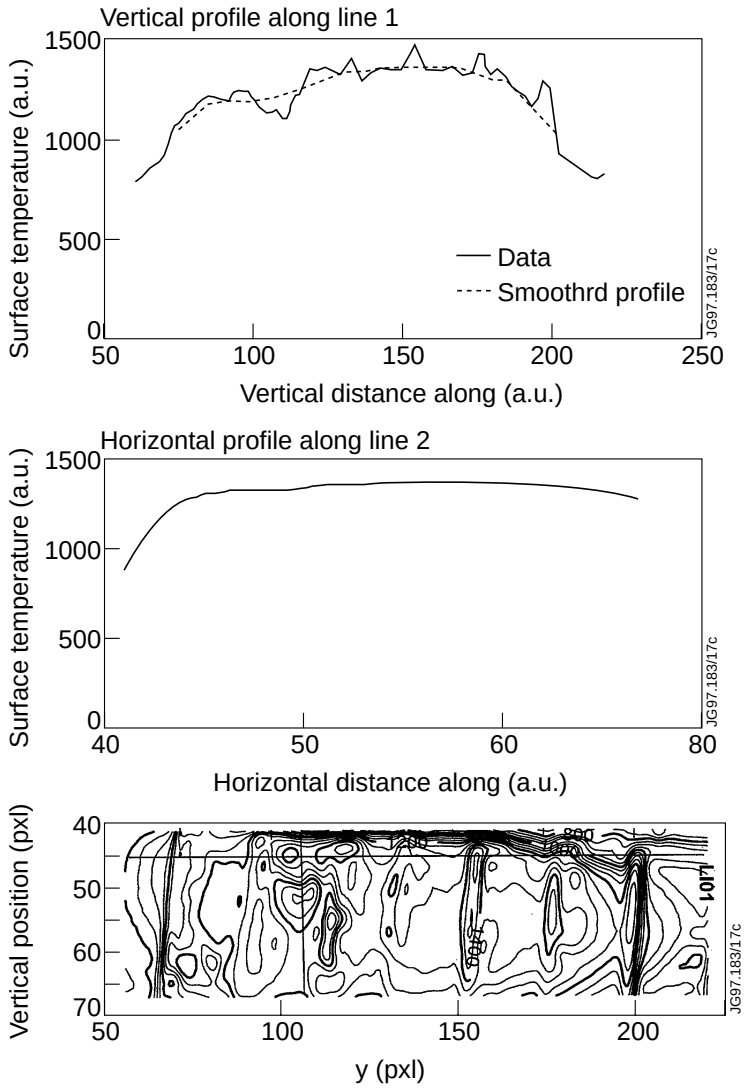

Fig.17: Temperature profiles during exposure of the Beryllium deposited on the copper calorimeter, bottom: contourplot of surface temperatures. Also shown are the lines 1 and 2 along which the profiles are shown.

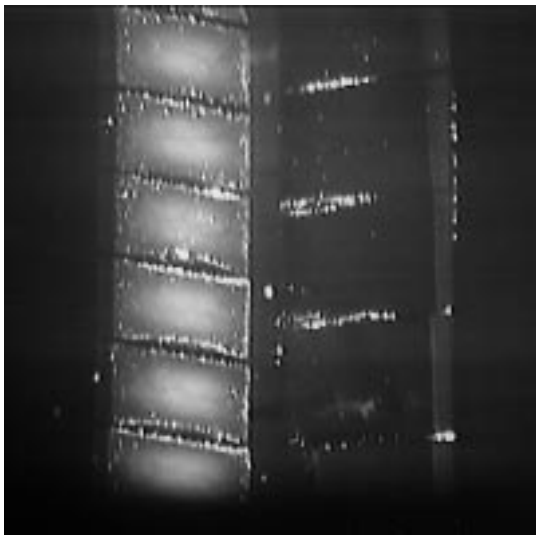

Fig.18: Videoprint of the test section and calorimeter during exposure. There are no hot spots on the deposited Beryllium. Pulse 88164, 11 MW/m^2.

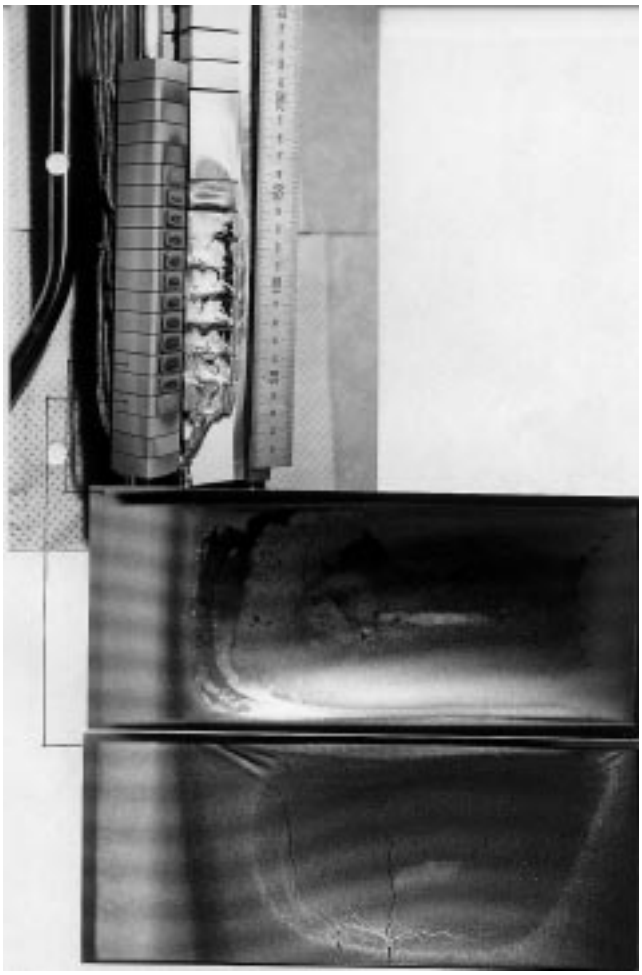

Fig.19: Test section at the end of part 2. The copper calorimeter shows substantial melting after a pulse with 11 MW/m^2 and 9 seconds. The Be monoblocks show clear signs of melting on 10 tiles, but no obvious cracks. There is also no sign that the molten Beryllium was flowing downwards.

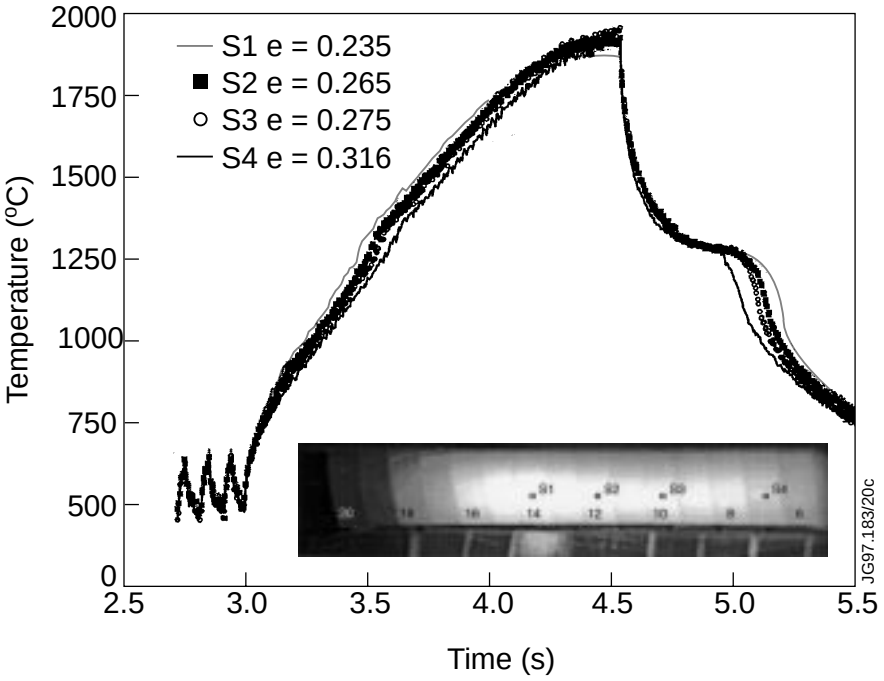

Fig.20: Surface temperatures of 4 spots in pulse 88150 with 22 MW/m^2. For each individual spot the emissivity is adjusted to force 1287 ^{0}C at the plateau during resolidification. The onset of melting and resolidification are clearly visible. Surface melting starts approximately 0.45 seconds after the start of unmodulated exposure.

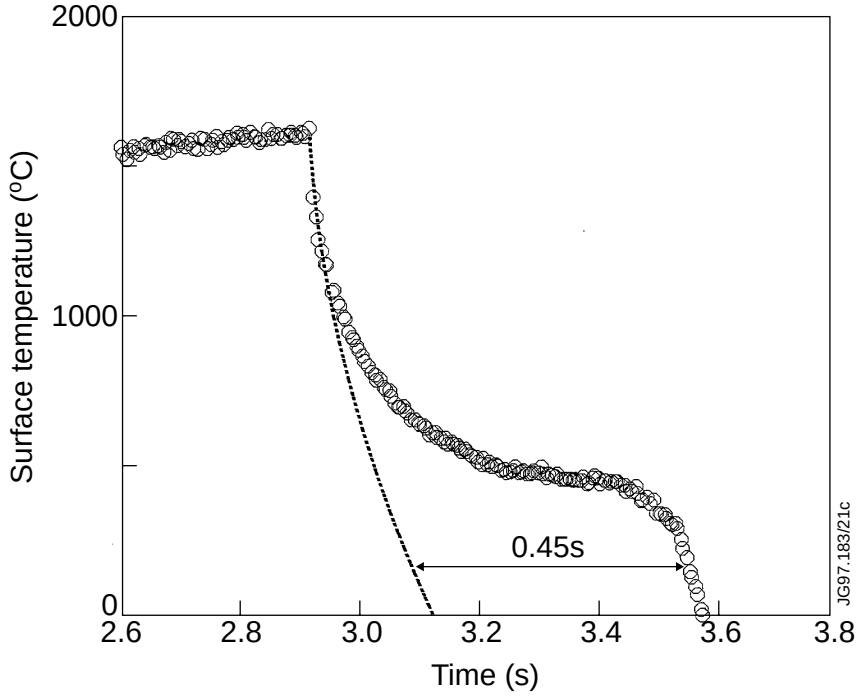

Fig.21: Delay in cooldown for spot 1. The delay due to resolidification takes 450 ms as estimated from the $\sqrt{time}$ *decay shown as dashed line.*

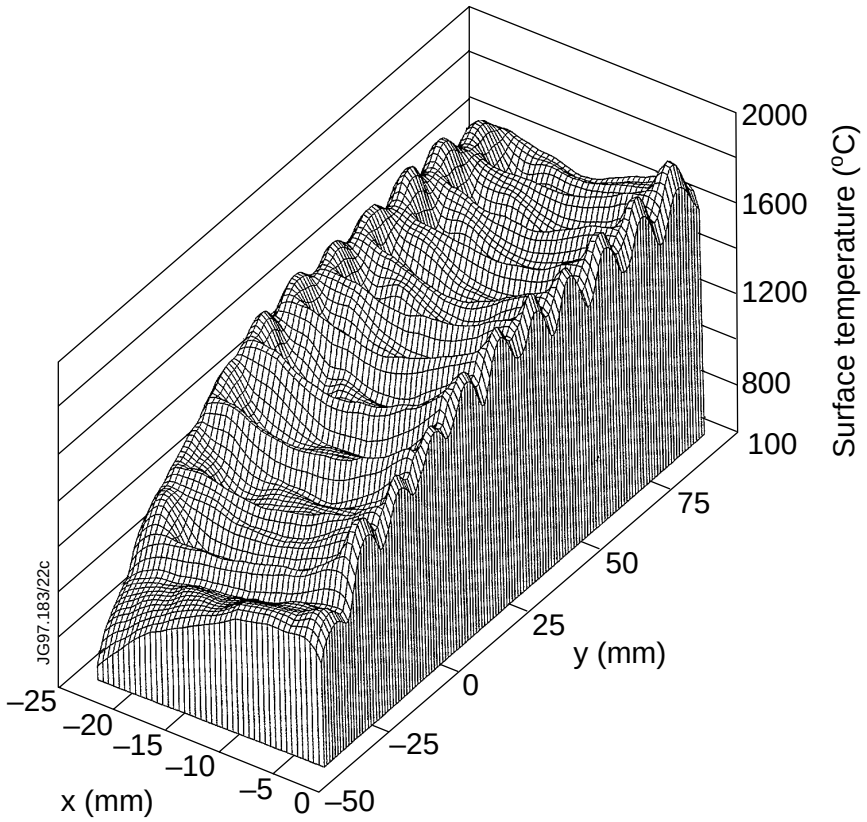

Fig.22: Surface temperatures during the last pulse (88165) with 11MW/m^2 , measured 6.5 seconds after start of exposure. Emissivity used: 0.1. The temperature distribution is complete distorted as the emissivity varies. The areas without surface melting appear hotter as they have a higher emissivity.

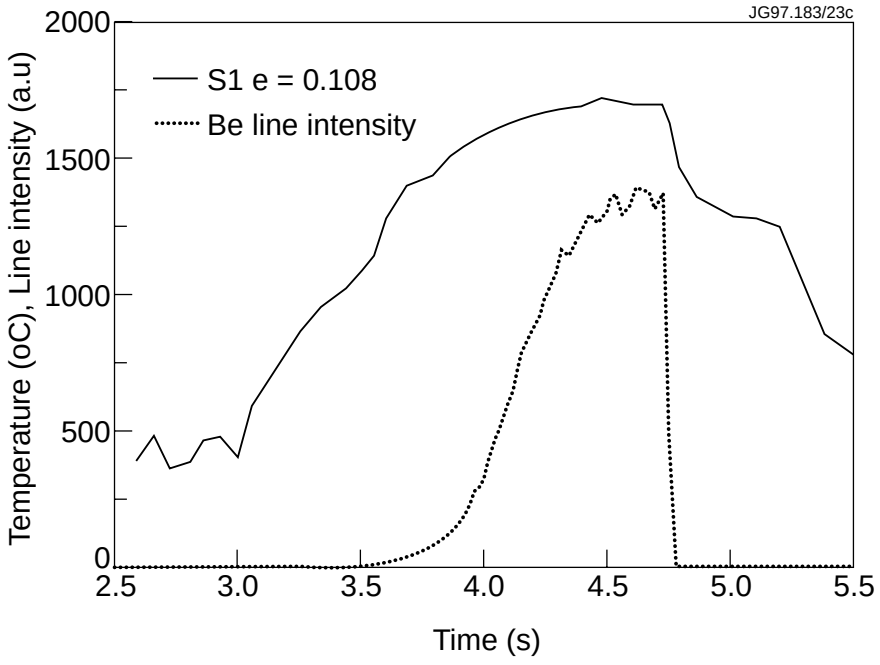

Fig.23: Surface temperature and intensity of the Be I line appear to get into equilibrium 1.5 seconds after exposure to full power. Pulse 88158 - part 2.

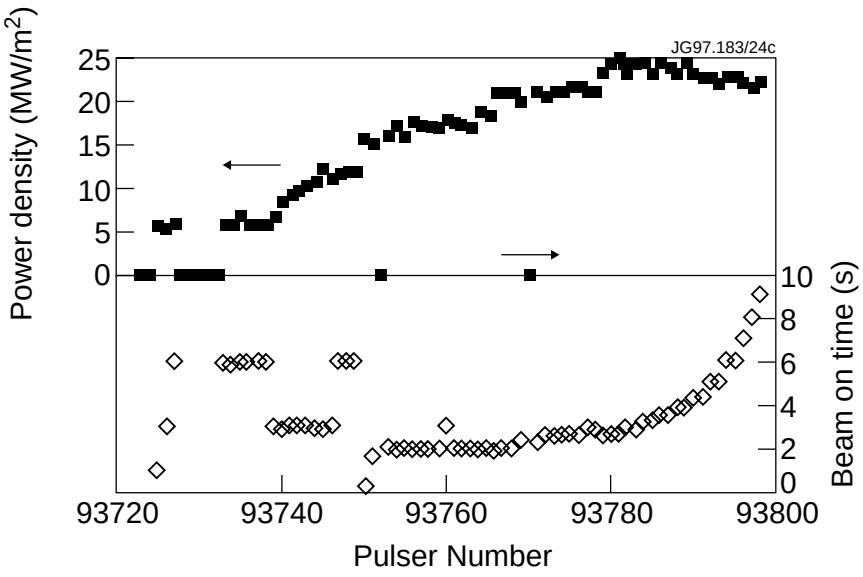

Fig.24: Power density and beam on time for part 3 (uncastellated monoblock with long melt exposure).

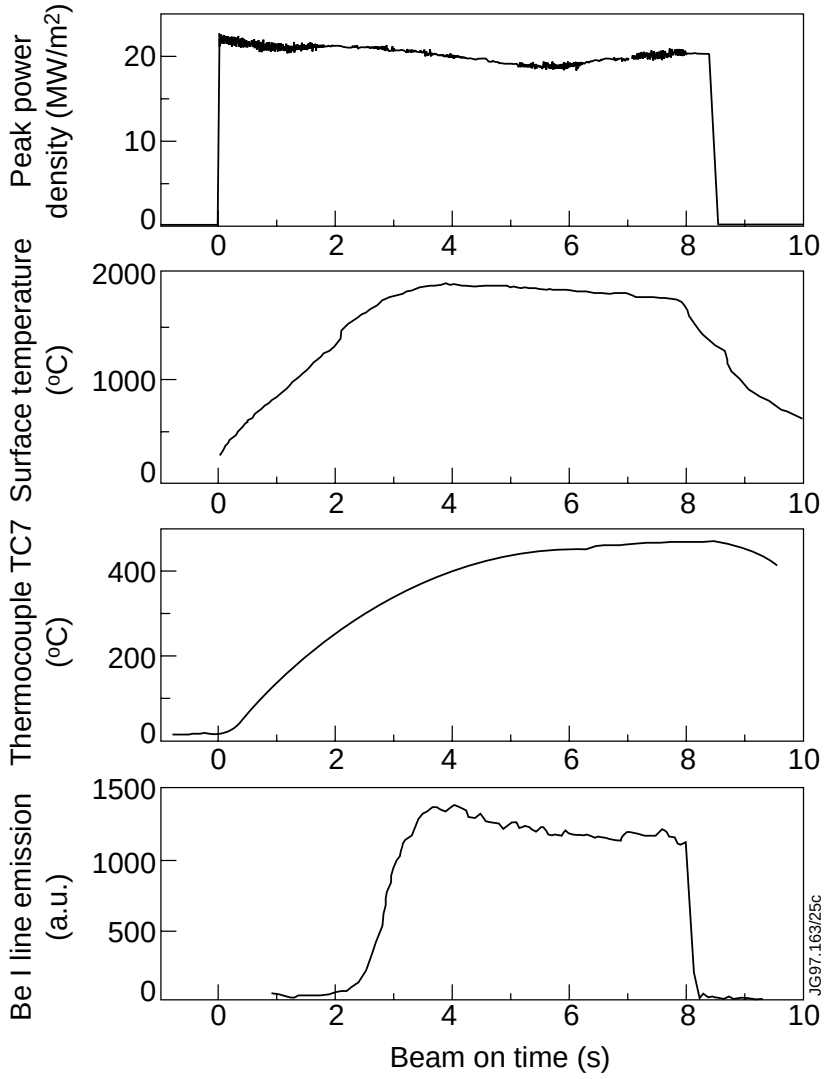

Fig.25: Temperature and Be line intensity for a 9 second pulse. Surface temperature and line intensity achieve equilibrium after 3.5 seconds. The power density (top) is reasonably constant. The thermocouple has a longer time constant than the surface temperature.

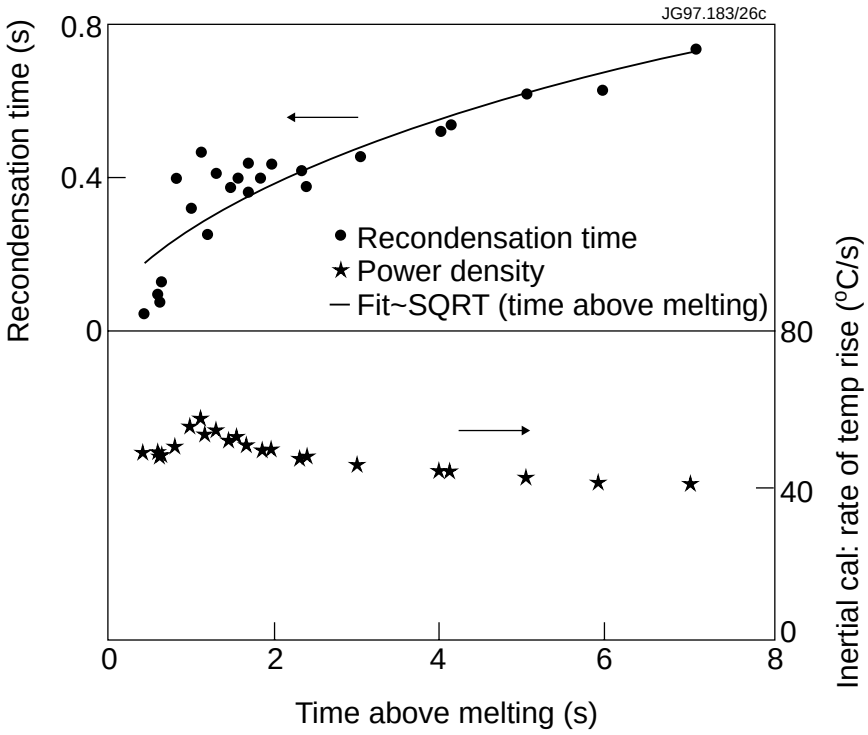

Fig.26: Recondensation time and power density for the long pulses. The recondensation time scales with $\sqrt{time}$.

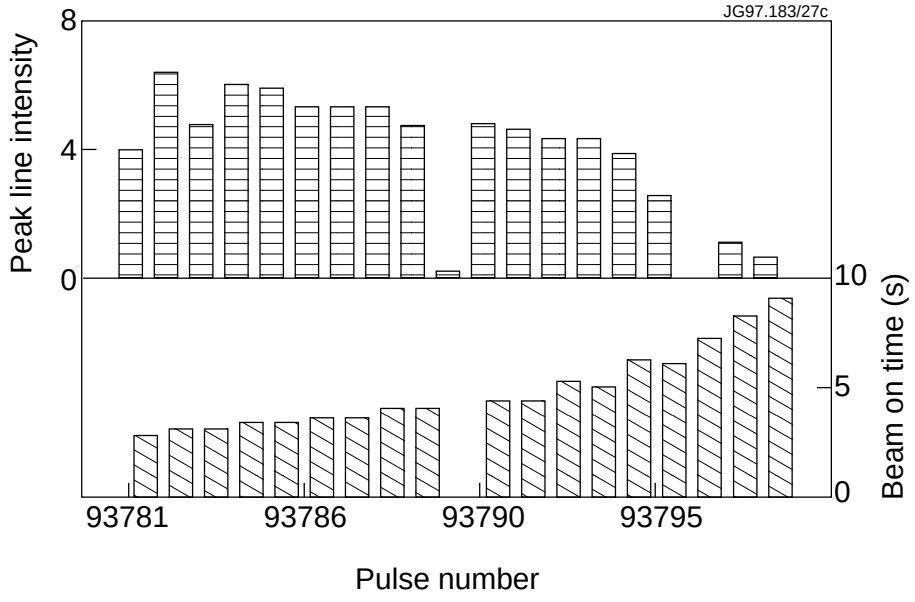

Fig.27: Attenuation of the line intensity due to coating of the window.

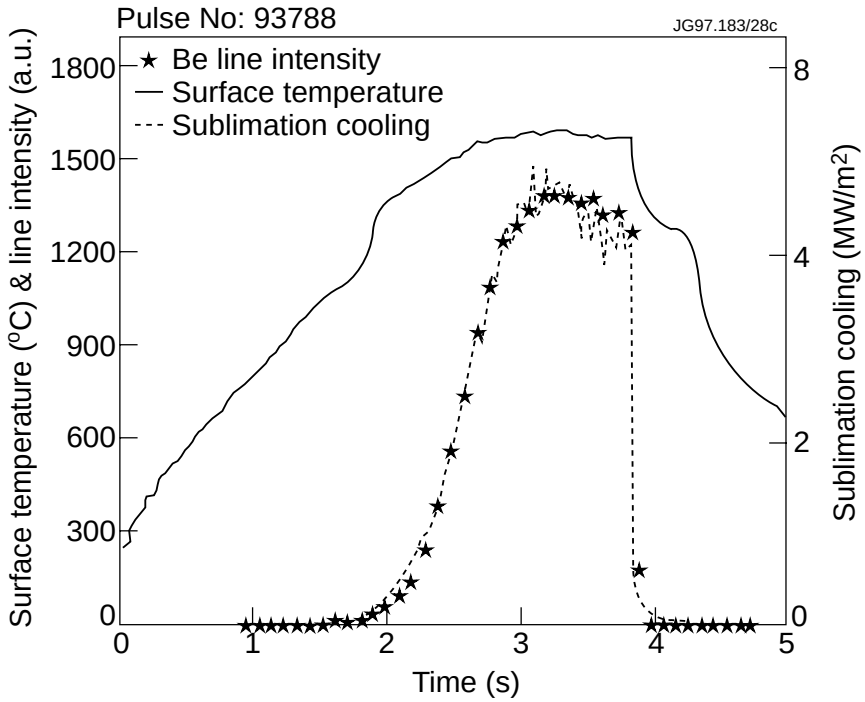

Fig.28: Comparison of Beryllium line intensity and sublimation rate calculated from the measured surface temperature.

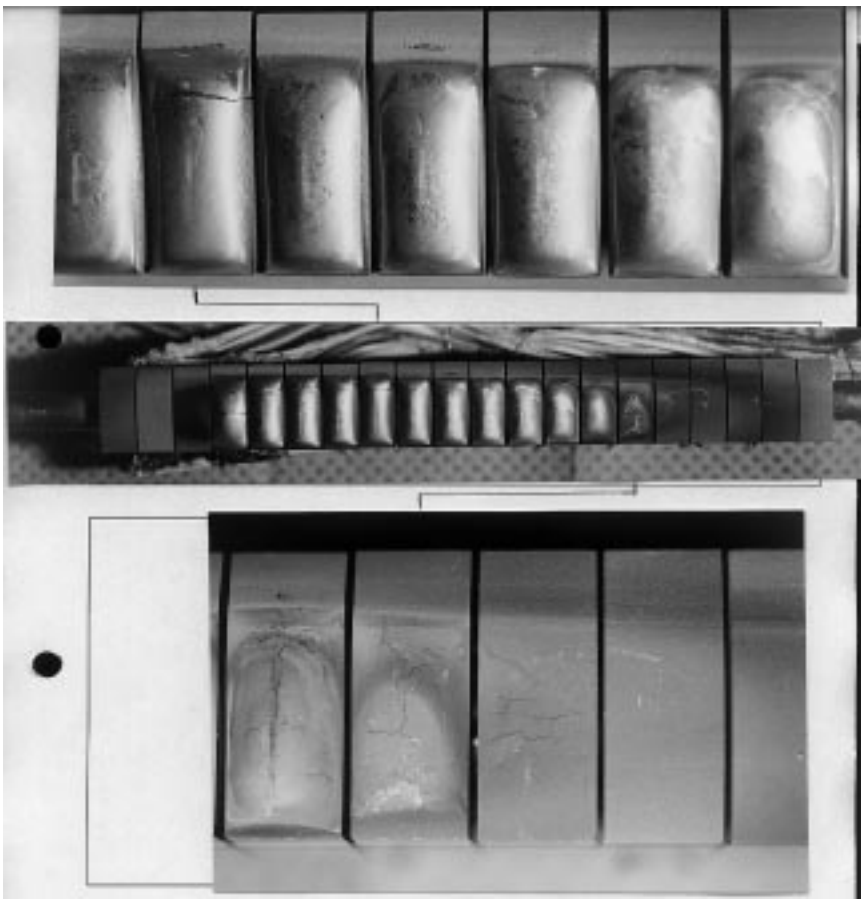

Fig.29: Beryllium tiles at the end of part 3 (extended melt scan). Two tiles have deep cracks (see insert top for detail) and tiles at the end of the melted area show surface cracks (bottom insert).

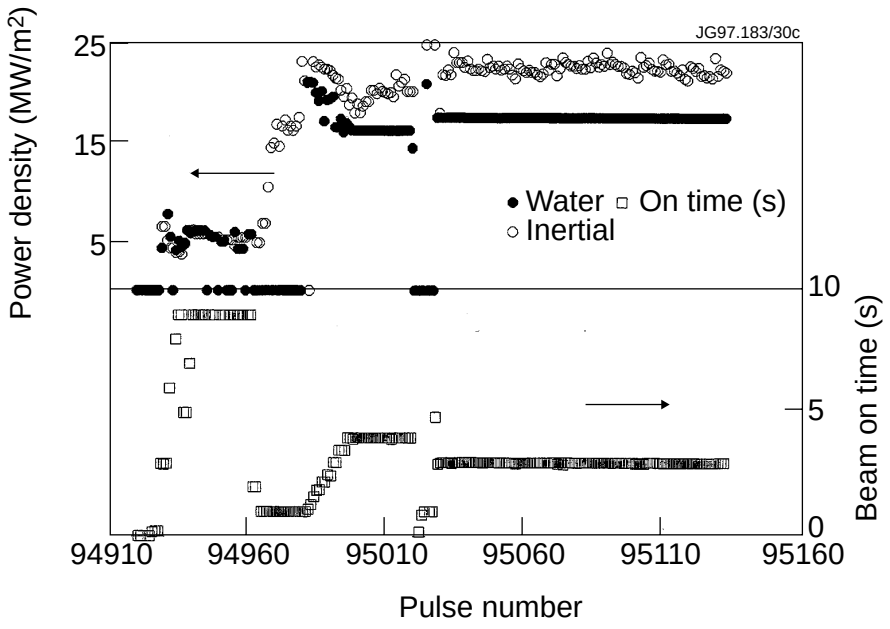

Fig.30: Power density and exposure time for part 4 (castellated monoblocks). Pulse length was mainly 3.5 and 4 seconds. The power density is approximately 20 MW/m^2 with approximately 130 significant pulses.

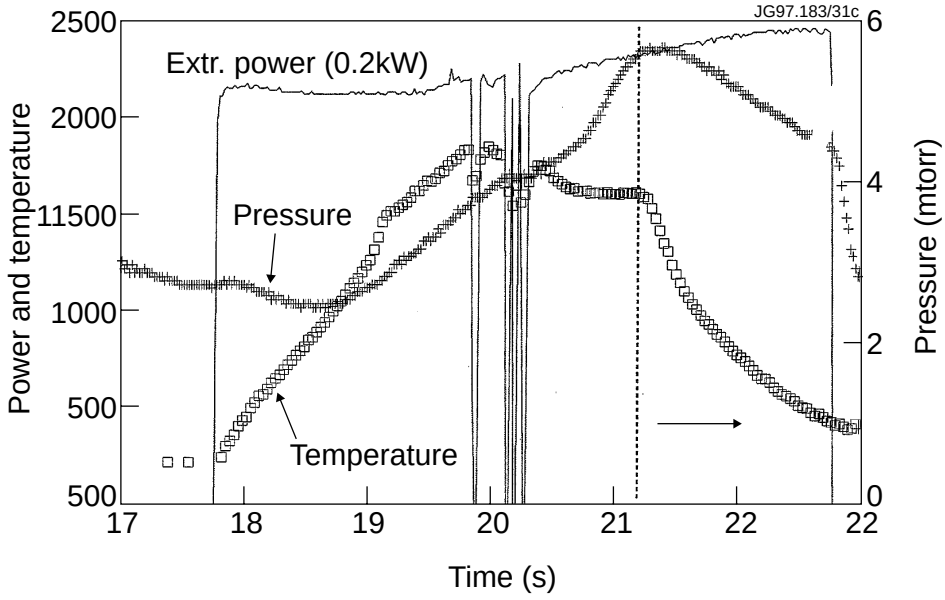

Fig.31: Loss of transmission in one pulse of 5 seconds duration. After 21 seconds the surface temperature drops dramatically and the tank pressure starts to fall. The power density is slightly rising.

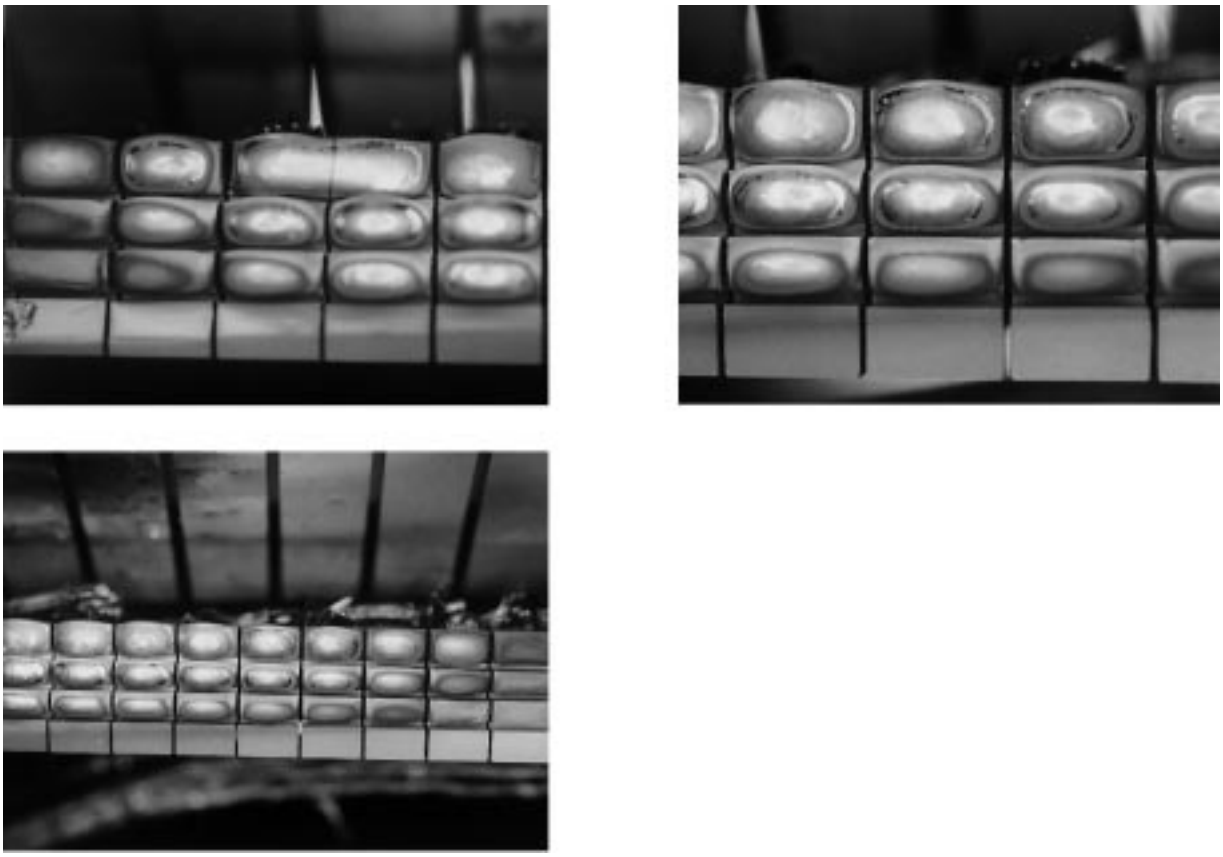

Fig.32: Castellated monoblocks after exposure. There are no signs of cracking.